Supporting Information

Dibenzyl Ether-Guided Microstructural Regulation of PtIrZn Catalysts for Ammonia Electrocatalysis

Zilan Jiang[a,b,d], Sibin zhu[a,d], Xufeng Tang[a,b,d], Haibo Tang[b], Xiaoming Zhu[c], Lun Yu[a,d], Letian Li[a,d], Yadong Wang[*,a,b,d], Haolin Tang[*,a,b,d], and Xiaoling Liu[*,c]

a. State Key Laboratory of Advanced Technology for Materials Synthesis and Processing, Wuhan University of Technology, Wuhan 430070, China

b. National Energy Key Laboratory for New Hydrogen-Ammonia Energy Technologies, Foshan Xianhu Laboratory, No. 1 Yangming Road, Danzao Town, Nanhai District, Foshan 528200, China

c. Hubei Key Laboratory of Radiation Chemistry and Functional Materials and School of Nuclear Technology and Chemistry & Biology, Hubei University of Science and Technology, Xianning 437100, China

d. Hubei Key Laboratory of Fuel Cell, Wuhan University of Technology, Wuhan 430070, China

***Corresponding author**

E-mail: ywang@whut.edu.cn, thln@whut.edu.cn, xiaolingliu@hbust.edu.cn.

Computational section：

First-principles calculations were performed within the density functional theory (DFT) framework, as implemented in the Vienna ab initio Simulation Package (VASP).[1,2] The core electrons were represented by the projector-augmented-wave (PAW) potential.[3,4] Generalized-gradient approximation (GGA) was used to determine the exchange-correlation potential.[5]

A 4×4 Pt supercell model with four layers was constructed, using the (100) or (111) surface as the interface. A 15 Å vacuum layer was introduced along the Z-axis to minimize interlayer interactions. Atoms in the bottom layer were fixed to simulate the bulk crystal structure. The plane wave cutoff energy of 400 eV and Γ-centered k-meshes with k-spacing of 0.3 $Å^{-1}$ were used for geometry optimization and static self-consistency (SCF). A 6×6×1 Monkhorst-Pack k-meshe was employed to sample the Brillouin zone for differential charge density and density of states (DOS). Electronic convergence and the geometry optimization force criterion were set to 10^{-5} eV and 0.01 eV $Å^{-1}$, respectively. All atoms, except those in the bottom layer, were fully relaxed until the total force on each atom converged to 0.03 eV $Å^{-1}$.

As a result, the reaction free energy (ΔG) was further calculated by the equation:

$$\Delta G = \Delta E_{DFT} + \Delta ZPE - T\Delta S + eU + 0.059\times \lg(pH) \qquad (S1)$$

where ΔE_{DFT} represents the reaction energy obtained from DFT calculation; ΔZPE is the phonone zero-point energy; TΔS is the change in the harmonic entropy contribution to the free energy and is obtained by calculating the partition function using vibrational frequencies; U is the applied potential (U = 0 or 0.3 V); and e is the charge transfer in each elementary step. Additionally, the thermodynamic corrections for all adsorbed and free species considered in this study were referenced from citation.[6] The visualization for all calculations was handled with the VESTA software.[7]

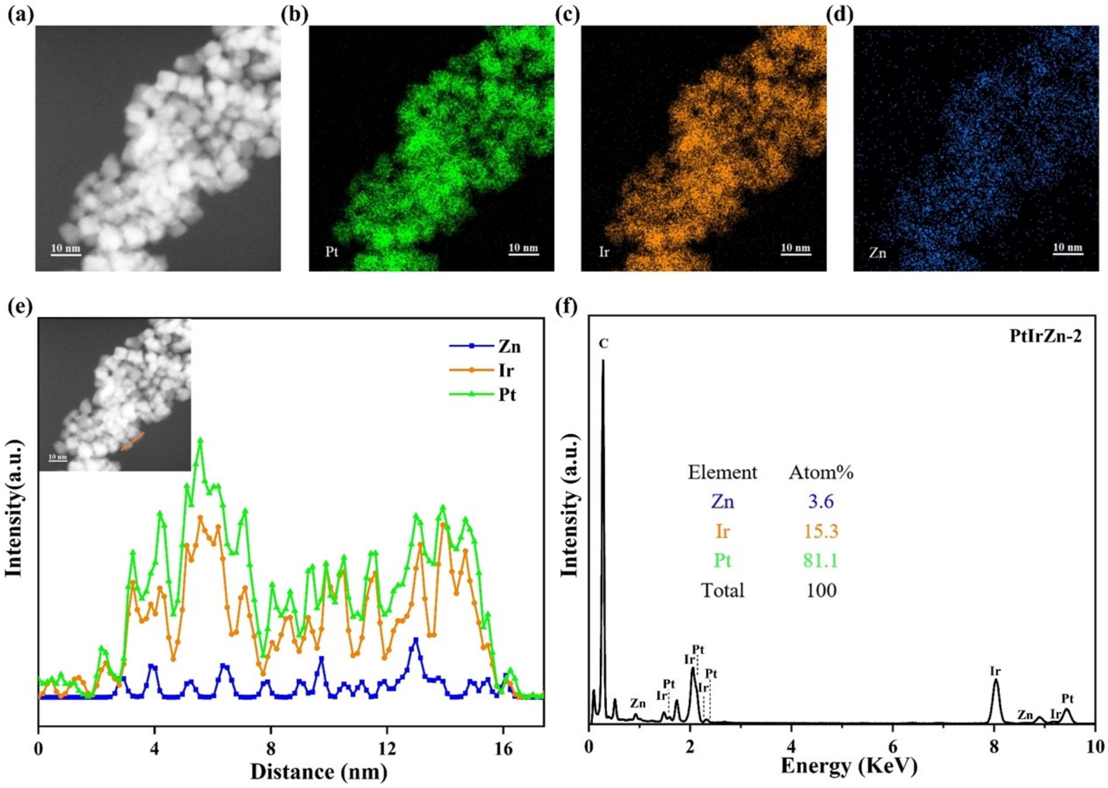

Fig. S1 (a) HAADF-TEM image of PtIrZn-2; (b)-(d) elemental mapping images illustrating the distribution of Pt, Ir, and Zn; (e) line-scanning profiles recorded across the orange line indicated in the inset; and (f) HAADF-TEM-EDX spectrum of PtIrZn-2.

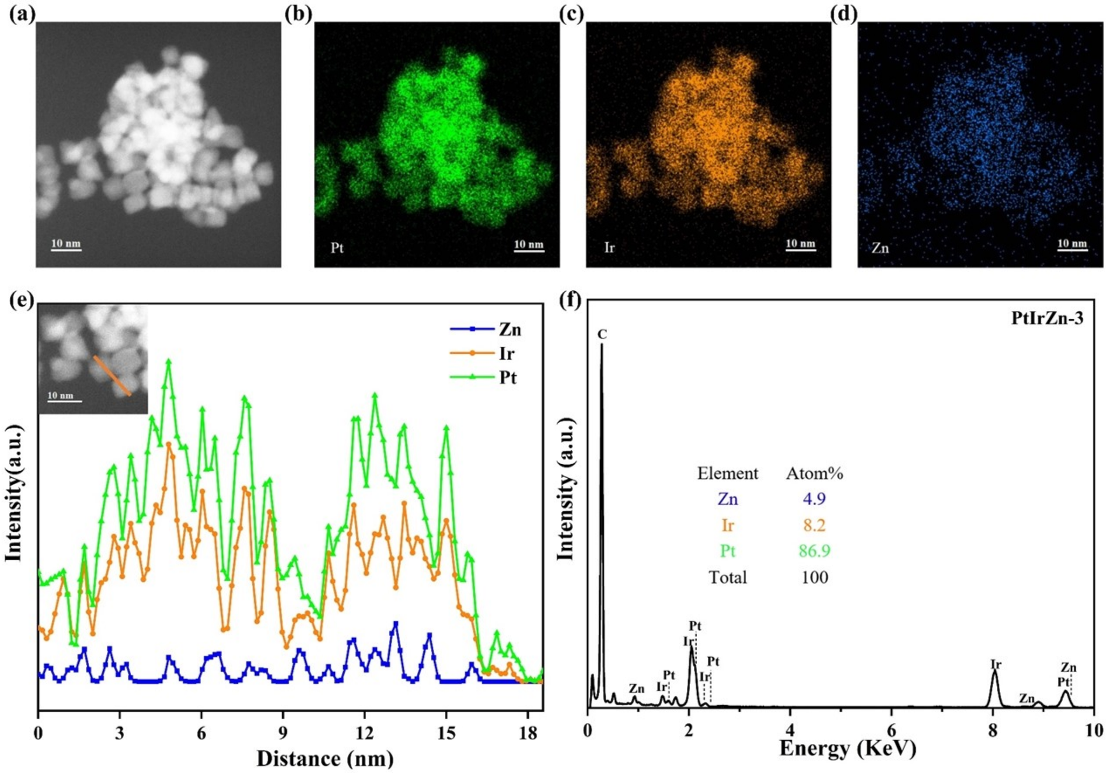

Fig. S2 (a) HAADF-TEM image of PtIrZn-3; (b)-(d) elemental mapping images illustrating the distribution of Pt, Ir, and Zn; (e) line-scanning profiles recorded across the orange line indicated in the inset; and (f) HAADF-TEM-EDX spectrum of PtIrZn-3.

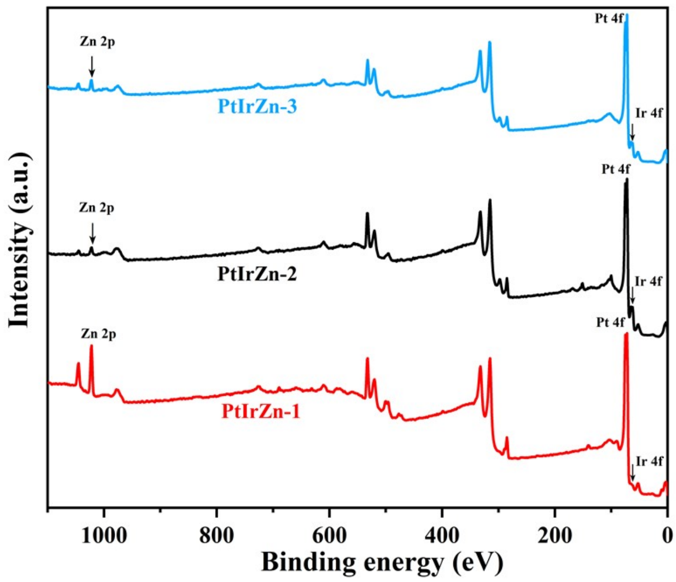

Fig. S3 XPS full-scan survey spectra of PtIrZn-1, PtIrZn-2, and PtIrZn-3.

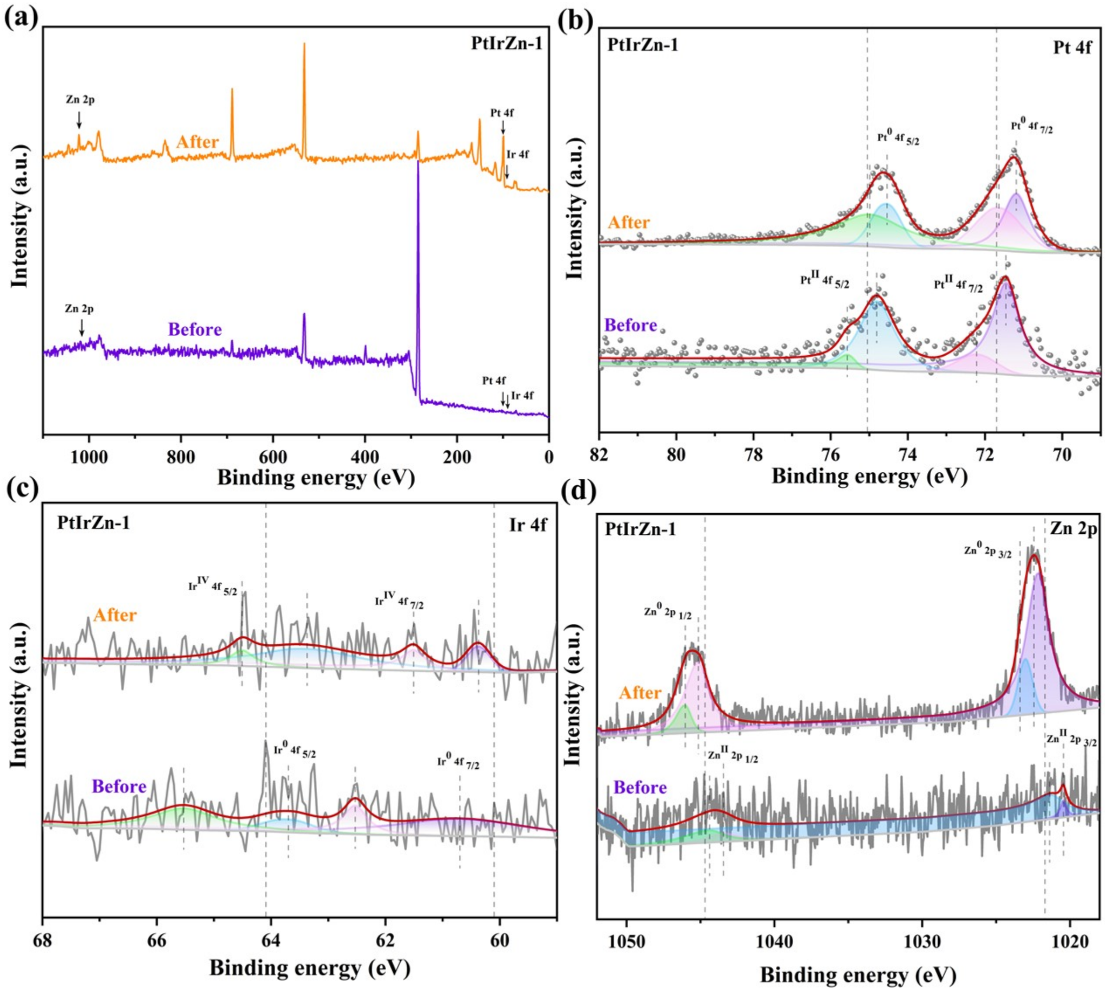

Fig. S4 (a) XPS full-scan survey spectra and high-resolution XPS spectra of Pt 4f (b), Ir 4f (c), and Zn 2p (d) for the PtIrZn-1 catalyst film before and after activation.

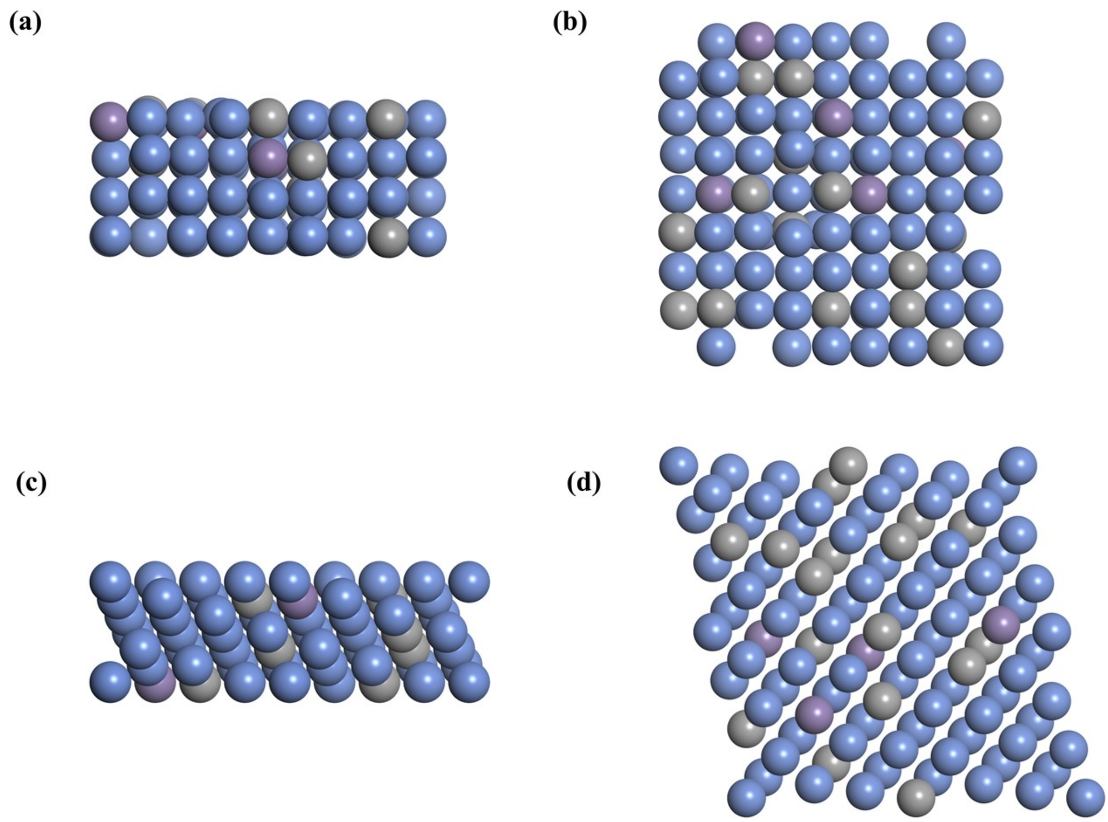

Fig. S5 DFT computational models: side view (a) and top view (b) of PtIrZn-1(100), and side view (c) and top view (d) of PtIrZn-1(111).

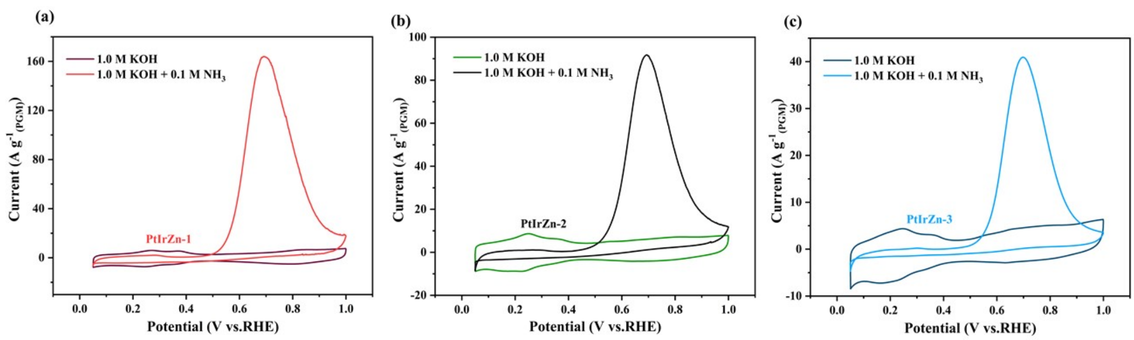

Fig. S6 CV s of PtIrZn-1 (a), PtIrZn-2 (b), and PtIrZn-3 (c) in 1 M KOH and 1 M KOH + 0.1 M NH_3.

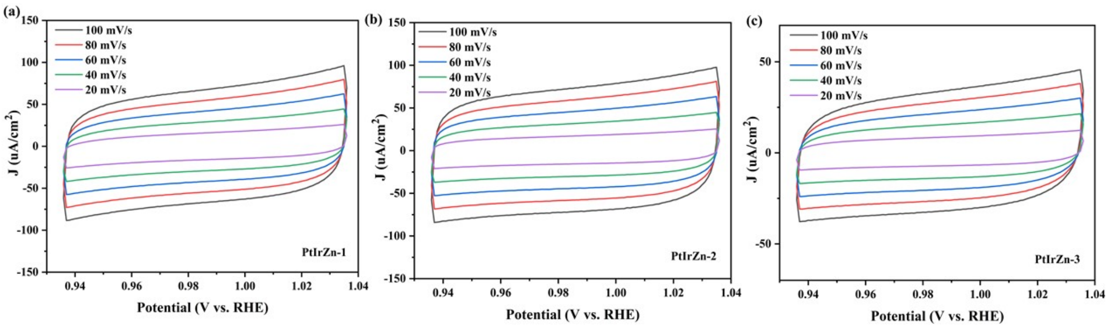

Fig. S7 CVs of PtIrZn-1 (a), PtIrZn-2 (b), and PtIrZn-3 (c) measured in 1 M KOH over the potential range of 0.94 to 1.04 V vs. RHE at various scan rates from 20 to 100 mV s^{-1}.

Table S1. Calculations Based on the Scherrer Equation.

Gauss	**Crystal Face**	**2Θ**	**B (rad)**	**D (nm)**	**D (nm)**	**A (nm)**	**V (nm^3)**	**ΔV (%)**
PtIrZn-1	(111)	40.1364	0.02669	**5.5**	**0.22448**	0.38880	0.05877	**2.66**
(number of iterations: 27)	(200)	46.6425	0.02746	**5.4**	**0.19457**	**-**	-	-
	(220)	68.1646	0.02623	**6.3**	**0.13746**	**-**	-	-
PtIrZn-2	(111)	39.9752	0.03197	**4.6**	**0.22535**	0.39030	0.05946	**1.53**
(number of iterations: 20)	(200)	46.4454	0.03694	**4.0**	**0.19535**	**-**	-	-
	(220)	67.8569	0.03808	**4.3**	**0.13800**	**-**	-	-
PtIrZn-3	(111)	39.8944	0.02718	**5.4**	**0.22579**	0.39106	0.05981	**0.95**
(number of iterations: 17)	(200)	46.4776	0.03556	**4.2**	**0.19522**	**-**	-	-
	(220)	67.8339	0.02976	**5.6**	**0.13805**	**-**	-	-

Note: K = 0.89, λ = 0.154056 nm, V_0 = 0.0604 nm^3;

Table S2. EIS Resistance Data.

Catalyst	R_s (Ω)	R_{ct} (Ω)
PtIrZn-1	6.405	518.9
PtIrZn-2	5.358	1218
PtIrZn-3	4.570	3070
commercial Pt/C	5.944	865
PtIr	8.923	8860
PtZn	4.503	5242

Reference:

1 G. Kresse and J. Furthmüller, *Computational Materials Science*, 1996, **6**, 15–50.

2 G. Kresse and J. Furthmüller, *Phys. Rev. B*, 1996, **54**, 11169–11186.

3 L. Lehtovaara, in *Fundamentals of Time-Dependent Density Functional Theory*, eds. M. A. L. Marques, N. T. Maitra, F. M. S. Nogueira, E. K. U. Gross and A. Rubio, Springer Berlin Heidelberg, Berlin, Heidelberg, 2012, vol. 837, pp. 391–400.

4 G. Kresse and D. Joubert, *Phys. Rev. B*, 1999, **59**, 1758–1775.

5 J. P. Perdew, K. Burke and M. Ernzerhof, *Phys. Rev. Lett.*, 1996, **77**, 3865–3868.

6 H. Zhang, L. Zhu, Y. Shen, M. Wu, T. Tian and H. Tang, *Adv Compos Hybrid Mater*, 2024, **7**, 46.

7 K. Momma and F. Izumi, *J Appl Crystallogr*, 2008, **41**, 653–658.